Citation: Clinical and Translational Gastroenterology (2011) 2, e3; doi:10.1038/ctg.2011.2

www.nature.com/ctg

Epithelial Gaps in a Rodent Model of Inflammatory Bowel Disease: A Quantitative Validation Study

Julia J. Liu, MD[1], Jan K. Rudzinski, BSc[1], Stephanie J. Mah[1], Aducio L. Thiesen, MD, PhD[2], Haiyu Bao[1], Eytan Wine, MD, PhD[3], Stephen C. Ogg, PhD[4], Pierre Boulanger, PhD[5], Richard N. Fedorak, MD[1] and Karen L. Madsen, PhD[1]

OBJECTIVES: Confocal laser endomicroscopy (CLE) is a non-invasive imaging modality of the gastrointestinal tract. Epithelial gaps in the small intestine of patients and rodents have been demonstrated using CLE. The goal of this study was to quantitatively validate the findings of epithelial gap density observed with CLE against confocal microscopy (CM) and light microscopy.

METHODS: Two strains of mice (control 129 Sv/Ev and interleukin 10 knockout (IL-10$^{-/-}$)) underwent CLE of the terminal ileum. Adjacent ileal tissues were examined using CM and light microscopy. The total number of gaps and cells in the villi were manually counted from the three-dimensional reconstruction of cross-sectional CLE and CM images. The histology specimens were reviewed for epithelial gap and cell counts by a pathologist blinded to the study groups. The inter- and intra-observer variability for cell and gap counts were determined.

RESULTS: For CLE, the gap densities (mean $\pm$ s.d.) in the ileum for control and IL-10$^{-/-}$ mice were: 9.5 $\pm$ 1.3 gaps per 1,000 cells and 20.6 $\pm$ 2.1 gaps per 1,000 cells counted ($P < 0.001$), respectively. For CM, the ileal gap densities were 7.3 $\pm$ 1.3 gaps per 1,000 cells and 22.8 $\pm$ 6.2 gaps per 1,000 cells ($P = 0.03$), respectively. For light microscopy, the ileal gap densities were 29.2 $\pm$ 5.9 gaps per 1,000 cells and 51.5 $\pm$ 6.4 gaps per 1,000 cells for the two strains.

CONCLUSIONS: CLE can be used to quantitatively assess epithelial cells and gaps with accuracy comparable to CM and light microscopy. In a mouse model of inflammatory bowel disease, the epithelial gap density in the terminal ileum is significantly increased when examined using all three modalities.

Clinical and Translational Gastroenterology (2011) **2,** e3; doi:10.1038/ctg.2011.2; published online 9 June 2011
Subject Category: inflammatory bowel disease

INTRODUCTION

Epithelial cell shedding is a normal physiological phenomenon that begins at the base of the crypts in the small intestine, in which epithelial cells arise from stem cells and mature. These cells then migrate up to the tip of the villi, whereupon they are eventually shedded.[1] This renewal process appears to be well conserved as it is seen even in organoids created from stem cells, in which epithelial cells were observed to continuously shed into the lumen as they are replaced, forming transient discontinuities in the epithelium, or epithelial gaps.[2] Emerging evidence suggests that epithelial cell shedding might represent another component to the epithelial barrier in the intestine.[1,3,4] Impaired barrier function has been implicated in the pathogenesis of inflammatory bowel disease (IBD).[5,6] Tumor necrosis factor (TNF)-α, a proinflammatory cytokine has been shown to increase epithelial cell shedding by as much as 20-fold,[3] in addition to increasing the permeability of small intestine to proteins, smaller solutes, and water in rodent models.[7,8] Furthermore, myosin light chain kinase—a key regulator of the actomyosin purse-string contraction wound closure mechanism in epithelial lining has been observed at the sites of physiological and pathological cell shedding.[9,10] Defects in the epithelial barrier can result in loss of tolerance to intestinal microbiota and ongoing inflammation, which are hallmarks of IBD. Recent studies suggest that epithelial gaps—discontinuities in the epithelial lining that result from epithelial cell shedding—may be an unexplored cause of barrier dysfunction.[1,3,4] Epithelial cell shedding induced by proinflammatory cytokines such as TNF-α can also promote inflammation and epithelial ulceration under certain conditions.[6,11]

Confocal laser endomicroscopy (CLE) is a novel, real-time imaging modality that enables three-dimensional (3-D) virtual optical biopsy *in vivo*.[12] Recently, epithelial gaps resulting from shedding of epithelial cells have been documented in the human small and large intestines using CLE.[3] Although epithelial gaps can be identified in real-time with little ambiguity, epithelial cell shedding occurs as a normal physiological process, therefore, qualitative description of the presence or absence of epithelial gaps is not sufficient to discern a diseased from a healthy state. A quantitative or semi-quantitative measurement of epithelial gaps is required to show any differences in the density of epithelial gaps

[1]Division of Gastroenterology, University of Alberta, Edmonton, Alberta, Canada; [2]Department of Laboratory Medicine and Pathology, University of Alberta, Edmonton, Alberta, Canada; [3]Department of Pediatrics, University of Alberta, Edmonton, Alberta, Canada; [4]Department of Medical Microbiology & Immunology, University of Alberta, Edmonton, Alberta, Canada; [5]Department of Computing Science, University of Alberta, Edmonton, Alberta, Canada
Correspondence: Julia J. Liu, MD, Division of Gastroenterology, University of Alberta, 1–10 Zeidler Ledcor Centre, Edmonton, Alberta, Canada T6R 2C1.
E-mail: julia.liu@ualberta.ca
Received 9 November 2011; accepted 27 April 2011

between healthy and diseased states. We have developed a quantitative measure of epithelial gaps seen on CLE, referred to as the epithelial gap density: the total number of epithelial gaps counted, normalized to the total number of epithelial cells counted on CLE images. This quantitative measure will need to be validated against well-accepted morphometric methods such as conventional confocal microscopy (CM) and/or light microscopy. In a pilot study, we have demonstrated increased epithelial gap density using CLE in patients with Crohn's disease, and a rodent model of IBD—the interleukin (IL)-10 knockout (IL-10$^{-/-}$) mice.[13] In a prospective, controlled study using probe-based CLE, we found that ulcerative pancolitis and severe clinical disease were seen in IBD patients with lower epithelial gap density.[14] Furthermore, very high gap density ($>$150 gaps per 1,000 cells) was observed only in Crohn's disease patients, and may be a discriminating feature for Crohn's patients.[14] Thus, determining epithelial gap density for IBD patients with CLE may have diagnostic and prognostic values.

In this study, we used CLE to quantitate the epithelial gap density in the small intestine of mice and validate the findings of CLE against conventional CM and light microscopy. Before CLE imaging, accurate histological identification of epithelial gaps has been limited by section and fixation artifacts, and conventional CM is not commonly available for routine clinical use. The introduction of CLE enabled unambiguous identification of epithelial gaps in patients.[3] For this validation, we examined a range of epithelial gap densities in two strains of mice, healthy controls (129 Sv/Ev mice) and a well-established IBD model, IL-10$^{-/-}$ mice.[15] To expand the range of epithelial gap densities, we added a third group, control 129 Sv/Ev mice treated with the proinflammatory cytokine TNF-α, which has been shown to induce epithelial cell shedding. In addition, we tested the inter- and intra-observer agreement for the quantification of epithelial cells and gaps.

METHODS

Animals. The mouse model of IBD used in this study was the IL-10$^{-/-}$ mouse, a homozygous IL-10-deficient strain generated on a 129 Sv/Ev genetic background.[15,16] These mice are a well-established rodent model for IBD. They do not develop colitis if raised under germ-free conditions,[16] and universally develop colitis (beginning at 8–12 weeks of age) if they are raised under conventional housing conditions.[15] In addition, these mice demonstrate increased small intestinal permeability before the onset of colitis.[15] Mice from the background 129 Sv/Ev strain were used as controls for all imaging experiments described below. IL-10$^{-/-}$ and 129 Sv/Ev aged between 24 and 28 weeks were used for experiments. The animals were housed in a temperature-controlled environment of 20–22 °C, with normal light–dark cycles of 12 h each. Animals were permitted free access to water and were fed standard chow. For the TNF-α treatment group, 20 μg of recombinant mouse TNF-α (Cedar Lane Laboratories, Burlington, NC) was reconstituted in sterile water. Each mouse received an intraperitoneal injection of 0.175 μg/g of body weight of TNF-α, at 4 h before CLE imaging. The study protocol was reviewed and approved by the Animal Care and Use Committee for Health Sciences at the University of Alberta.

Sample size calculation. The sample size calculation was performed for the comparison of 129 Sv/Ev controls and IL-10 knockout mice housed in standard conditions. For the IL-10$^{-/-}$ mice, the variability estimated from the sample size in the previous study was s.d. of 5, the mean epithelial gap density was 17.6 gaps per 1,000 cells. For the 129 Sv/Ev controls, the mean epithelial gap density was 10.5 gaps per 1,000 cells. To ensure a statistical power of at least 0.8 and an alpha of 0.05, a total of eight mice were needed in each group for the comparison of the two groups. We chose to use 10 mice in each group for this correlation study.

Confocal laser endomicroscopy. We used a single-photon rigid confocal endomicroscope (Five 1 Fluorescence *In Vivo* Confocal Endomicroscopy System, Optiscan, Victoria, Australia) to image the terminal ileum of the rodents.[3] The confocal endomicroscopy systems are single photon, as beam dispersion prevents imaging with femtosecond pulse to photon microscopy system. The confocal endomicroscope delivers an excitation laser wavelength of 488 nm. Each cross-sectional image has a field of view of 500 μm by 500 μm, the optical slice is 7 μm in thickness, and the lateral resolution of the endomicroscope is 0.7 μm (the diameter of an erythrocyte is between 6 and 8 μm).

Mouse surgery. Mice were anesthetized with a ketamine and xylazine mixture (10 μl/g) intraperitoneally. A 2-cm segment of the small intestine was exteriorized with previously described methods,[3] the lumen was cut open on the anti-mesenteric surface, the intestinal tissue was then flushed with normal saline, and topical acriflavine was applied. Topical acriflavine was chosen as a staining agent as it is a nuclear stain that was previously used by other investigators for the identification of epithelial gaps in the rodent model.[3] In addition, the duration of florescence achieved using acriflavine is much longer than intravenous fluorescein, in addition to ease of administration. The intensity of the acriflavine stain is stable for the duration of confocal endomicroscopy, and fluorescein has been shown to dissipate within 20 min of administration. After the excess acriflavine was washed off, CLE was performed using the rigid confocal mini-microscope; approximately 25 cross-sectional images were obtained per tissue section. Movement artifacts from intestinal smooth muscle contraction were minimized by pinning the exteriorized intestinal tissue to a corkboard. Motion artifacts from cardiac or respiratory cycles were controlled by spatially removing the intestinal tissue away from the thorax. Using the above methods, we were able to acquire cross-sectional images that were sufficiently free of movement artifacts for 3-D reconstruction.

The cross-sectional images were then digitally aligned and the features extrapolated to create a surface relief of the relevant segment of the small intestine. Interpolation of the two-dimensional (2-D) frames in each stack was performed by an imaging expert (P.B.) using a feature-guided, shape-based

image reconstruction software (VolView 3.0, Kitware, Clifton Park, NY). The 3-D relief images were then analyzed to quantify for epithelial gaps by a reviewer blinded to the status of the animal. Epithelial gaps and cells were manually counted in at least five villi per animal for the calculation of epithelial gap density.

Confocal microscopy. For identification of epithelial gaps with multi-photon confocal microsocopy, we used a combination of a nuclear stain (DAPI or 4′,6-diamidino-2-phenylindole) and an actin stain (phalloidin). DAPI stain forms fluorescent complexes with natural double-stranded DNA showing fluorescence specificity for the nucleus.[17] Phalloidin bicyclic heptapeptide binds to actin filaments and hence is used for identification of the cytoskeletons that are present in cells.[18] We used phalloidin coupled with Alexa568 to stain for cytosolic actin. Thus, we defined spaces in between cells that are devoid of nuclear and stain as epithelial gaps. These spaces appear as irregularly shaped, hypodense areas using the combined DAPI and phalloidin imaging.

Mouse terminal ileum tissue was excised and fixed overnight at 4 °C in 4% paraformaldehyde freshly prepared in phosphate-buffered saline (PBS). Tissue was stained and mounted for imaging using a slightly modified version of the protocol by Appleton *et al*.[19] Briefly, fixed intestinal tissue was cut into 2 mm lengths and rinsed three times in PBS, permeabilized for 2 h at room temperature (1% Triton-X100 in PBS), rinsed 3×15 min in PBS, and blocked to prevent nonspecific staining for 1 h slowly rocking at room temperature (1% bovine serum albumin, 3% normal goat serum, 0.2% Triton-X100 in PBS). Individual pieces of tissue were stained overnight while slowly rocking at 4 °C in 1.5-ml microcentrifuge Eppendorf tubes containing 1 ml of staining buffer (0.1% bovine serum albumin, 0.3% normal goat serum, 0.2% Triton-X100 in PBS) plus 5 μg/ml of DAPI and where indicated 0.1 U/ml of Alexa568-coupled phalloidin. Excess fluorochrome was removed by rinsing 3×50-ml PBS rinses, 1 h per rinse, before mounting in 97% 2,2′-thiodiethanol. Mounting was achieved by immersing the samples in increasingly concentrated dilutions of 2,2′-thiodiethanol (10, 25, 50, and 97%) as previously described.[20] At each dilution, samples were slowly rocked at 4 °C for 2 h. Samples were left in 97% 2,2′-thiodiethanol overnight before imaging. Samples were mounted in 35-mm tissue culture dishes fitted with coverslip bottoms 170-μm thick (Number 1.5) (WillCo-Dish, Willco Wells, Amsterdam, The Netherlands). A few drops of 97% 2,2′-thiodiethanol were used to cover the tissue, which was held in place by placing a top-mounted coverslip (12-mm diameter).

Confocal microscopy imaging of the villi was carried out using a Quorum WaveFX spinning disk confocal microscope (Quorum Technologies, Guelph, CA). This system integrates the Yokogawa CSU-X1 confocal scan unit (Yokogawa Electronics, Tokyo, Japan) and an Olympus IX-81 microscope base (Olympus Canada, Markham, Canada). Excitation was provided by a 405-nm laser for DAPI, and a 561-nm laser for Alexa-568. The objective lens was an Olympus $\times 10$, 0.3NA ($\times 10$ UPLFLN, W.D. 10 mm). Images were captured on a Hamamatsu ImagEM EMCCD camera (Hamamatsu Photonics, Hamamatsu City, Japan). Control of all electronic shutters, filters, microscope components, and camera was coordinated through Metamorph (Molecular Devices, Sunnyvale, CA).

The 3-D CM images were then analyzed for epithelial gaps and cells by a blinded reviewer. Epithelial gaps and cells were manually counted in a minimum of five villi per animal for the calculation of epithelial gap density.

Light microscopy. The terminal ileum adjacent to areas imaged with confocal endomicroscopy was excised for light microscopy examination. The ileal tissue was gently washed with normal saline at room temperature, cut into 5×5 mm sections, and placed in Cryomatrix (Thermo Scientific, Pittsburgh, PA) medium for frozen sectioning. The intestinal tissue block was sectioned at 5 μm in cryostat microtome at −20 °C, with special attention given to preserve the fragile structures in the block. The frozen sections were then stained with hematoxlyn and eosin, alcian blue, and nuclear fast red to differentiate epithelial gaps from goblet cells, providing sufficient contrast to facilitate cell and gap counting. Epithelial gaps on light microscopy-prepared specimens appeared as spaces observed in between cells that were not stained with either alcian blue or nuclear fast red. The histological specimens were reviewed by an expert gastrointestinal pathologist blinded to the status of the animal. Epithelial gaps and cells were manually counted in 10 villi per animal for the calculation of epithelial gap density.

Inter- and intra-observer agreement. CLE and CM images were reviewed by two independent reviewers for manual counting of epithelial cells and gaps. Criteria for epithelial gaps seen on CLE were adopted from two criteria that were previously reported by Kiesslich *et al*.[7] First, epithelial gaps do not contain a nucleus, and second, the gaps appear relatively uniform from all angles of view. Furthermore, on 3-D reconstructed images, the hypodense area does not change in density at different views. The two reviewers were trained by an expert confocal endomicroscopist and an expert confocal microscopist for counting of 25 villi, before counting the images independently. For the inter-observer agreement study, the two reviewers were given CLE and CM images of the villi for counting of cells and gaps, without knowledge of the histology or the results of the other reviewer. For the determination of intra-observer agreement, one of the two reviewers recounted epithelial cells and gaps at 1 month following the initial count. The counts from the two reviewers were collected separately and analyzed for agreement.

Statistical analysis. We performed analysis of continuous variables using the Wilcoxon rank-sum test with the STATA data analysis and statistical software (StataCorp LP, College Station, TX). Each continuous variable was expressed as the mean value ± s.d. A *P*-value of <0.05 was considered significant; all tests were two-tailed. For each set of paired CLE and CM gap densities, we assessed the correspondence between the gap densities observed by the two modalities, which was calculated using the Spearman's rank

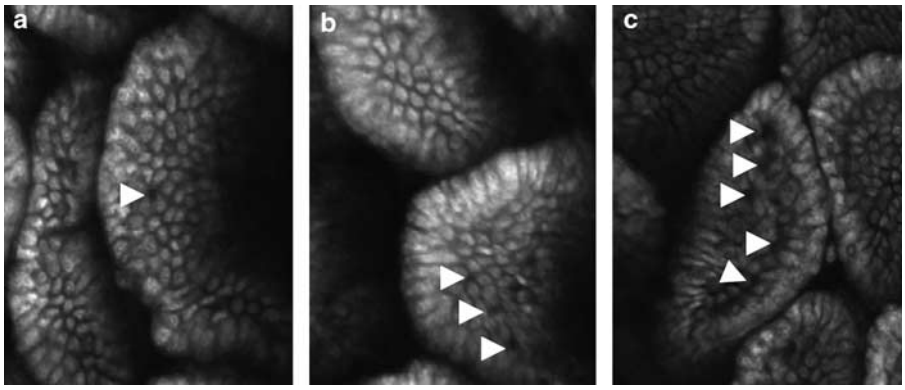

Figure 1 Representative confocal laser endomicroscopy images of the mouse ileum. The *en face* view of villi showing the presence of epithelial gaps in control (**a**), IL-10$^{-/-}$ (**b**), and tumor necrosis factor (TNF)-α-treated control (**c**) mice, respectively. Epithelial gaps appear as hypodense, irregularly shaped spaces in the intestinal lining, indicated by white arrowheads. Scale bar = 20 μm.

correlation, along with 95% confidence intervals (CIs). For the inter-observer (observer 1 vs. observer 2) and intra-observer (time 1 vs. time 2) agreement studies, the correspondence between the two sets of paired observations were assessed by calculating Spearman's rank correlation, along with 95% CIs.

RESULTS

Confocal laser endomicroscopy. The goal of our study was to quantitatively validate the findings of epithelial gap density observed using CLE against conventional CM and light microscopy. For better identification of epithelial gaps, we performed 3-D reconstructions of the 2-D cross-sectional images of mouse ileum. These 3-D reconstructed images allowed easier differentiation of epithelial gaps from goblet cells, using criteria previously developed by Kiesslich *et al*.[3] Adequately imaged villi, defined as *en face* villi images showing 75% of villi surfaces on the CLE images, were used for counting of epithelial cells and gaps. A minimum of five villi from each animal were manually counted; the gap density per 1,000 cells was calculated from the total number of epithelial gaps divided by the total number of epithelial cells. CLE was performed in control mice ($n = 10$), IL-10$^{-/-}$ mice ($n = 10$), and TNF-α-treated control mice ($n = 3$). Representative CLE images from control, IL-10$^{-/-}$, and TNF-α-treated mice are shown in Figure 1. The mean gap density was 9.5 ± 1.3 gaps per 1,000 cells for the control 129 Sv/Ev mice. The mean gap density of 20.6 ± 2.1 gaps per 1,000 cells ($P < 0.001$) in the IL-10$^{-/-}$ mice was significantly higher than controls. The mean gap density for the TNF-α-treated mice was also significantly higher than controls: 47.1 ± 4.3 gaps per 1,000 cells ($P < 0.00001$). Epithelial gap densities for the three groups of study mice seen on CLE are shown in Figure 2.

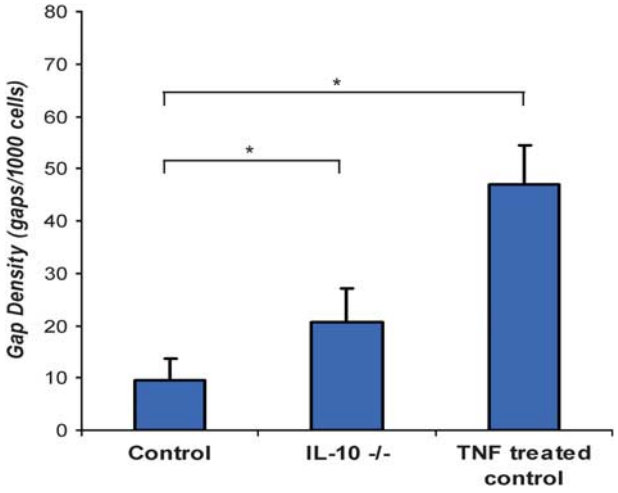

Figure 2 Epithelial gap densities for control 129 Sv/Ev, IL-10$^{-/-}$, and tumor necrosis factor (TNF)-α-treated control mice (mean values ± s.d.) using confocal laser endomicroscopy. The *P*-values for comparison of the means were determined using Wilcoxon signed-rank test. * indicate $P < 0.001$.

Confocal microscopy. For multi-photon CM, 3-D reconstructions of the 2-D cross-sectional images at 1-μm intervals were performed. Epithelial gaps were identified as irregularly shaped, hypodense areas seen on the combined DAPI and phalloidin imaging. Cell counts on CM imaging were derived from the nuclear counts seen on DAPI stain. Ileal tissues adjacent to CLE imaging from the control mice ($n = 10$), IL-10$^{-/-}$ mice ($n = 10$), and TNF-α-treated control mice ($n = 3$) were examined using multi-photon CM. Representative CM images from control, IL-10$^{-/-}$, and TNF-α-treated mice are shown in Figure 3. The mean gap density was 7.3 ± 1.3 gaps per 1,000 cells for the 129 Sv/Ev mice, whereas a higher gap density was observed in the IL-10$^{-/-}$ mice at 22.8 ± 6.2 gaps per 1,000 cells ($P = 0.03$), and TNF-α-treated 129 Sv/Ev mice at 32.6 ± 2.9 gaps per 1,000 cells ($P < 0.001$). Epithelial gap densities for the three groups of study mice seen on CM are shown in Figure 4.

The correlation of the CLE to CM findings was determined using the non-parametric Spearman's correlation coefficient. The correlation coefficient was 0.88 for gap densities determined using the two methods, with the upper and lower limits of the 95% CI being 0.72 and 0.95, respectively. The correlation of CLE to CM findings is shown in Figure 5.

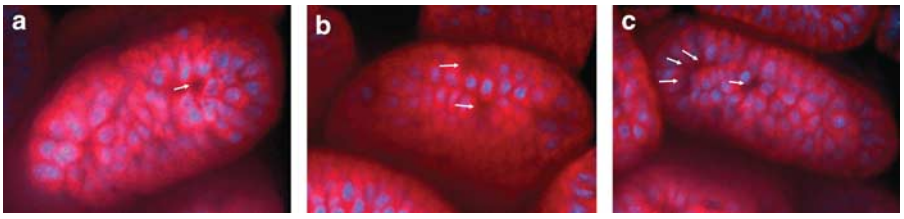

Figure 3 Representative confocal microscopy images of the mouse ileum. Representative images overlying 4′,6-diamidino-2-phenylindole (DAPI) and phalloidin of the villi showing epithelial gaps in the ileum of control (**a**), IL-10$^{-/-}$ (**b**), and tumor necrosis factor (TNF)-α-treated control (**c**) mice, respectively. Epithelial cell nuclei appear blue; epithelial gaps appear as hypodense, irregularly shaped spaces in the DAPI and phalloidin overlay images. Epithelial gaps are indicated by white arrowheads.

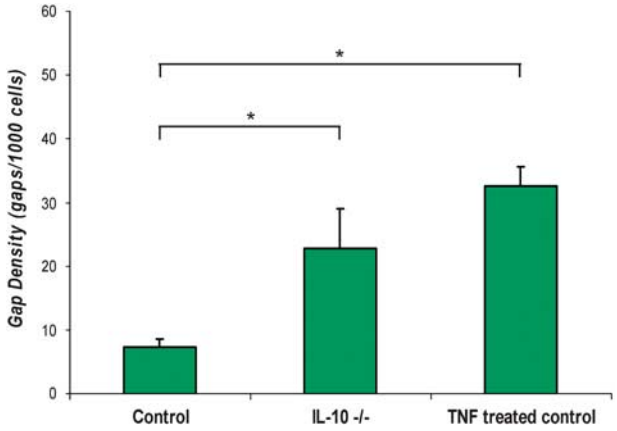

Figure 4 Epithelial gap densities for control 129 Sv/Ev, IL-10$^{-/-}$ and tumor necrosis factor (TNF)-α-treated control mice (mean values ± s.d.) with multi-photon confocal microscopy stained with 4′,6-diamidino-2-phenylindole (DAPI) and phalloidin. The *P*-values for comparison of the means are from Wilcoxon signed-rank test. * indicate $P \leq 0.03$.

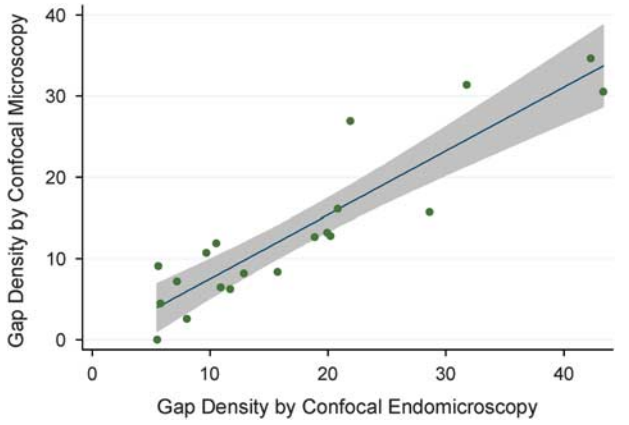

Figure 5 Correlation of epithelial gap densities for control 129 Sv/Ev, IL-10$^{-/-}$, and tumor necrosis factor (TNF)-α-treated control mice using confocal laser endomicroscopy to conventional confocal microscopy. The 95% confidence bands are shown.

Light microscopy. Epithelial gaps observed using light microscopy appear as spaces observed in between cells that do not stain with alcian blue/nuclear fast red. Ileal tissues adjacent to CLE-imaged areas from the control mice ($n = 10$), IL-10$^{-/-}$ mice ($n = 10$), and TNF-α-treated control mice ($n = 3$) were fixed in cryomedium, sectioned, stained with alcian blue and nuclear fast red, and hematoxylyn and eosin for light microscopy examination. Representative light microscopy images from control, IL-10$^{-/-}$, and TNF-α-treated mice are shown in Figure 6. The epithelial gap density seen using light microscopy in the control 129 Sv/Ev mice was 29.2 ± 5.9 gaps per 1,000 cells counted, or 2.92% of cell spaces. This is comparable to previous report in which morphometric analysis showed 3% of cell positions were epithelial gaps.[1] Our findings confirm previous reports in the control animal model. The gap density is significantly increased in the IL-10$^{-/-}$ mice to 51.5 ± 6.4 gaps per 1,000 cells counted ($P < 0.0001$). Similarly TNF-α-treated control animals also have an increased epithelial gap density at 64.5 ± 6.1 gaps per 1,000 cells counted ($P < 0.00001$). The epithelial gap densities for the three groups of study mice as per light microscopy are shown in Figure 7.

Inter- and intra-observer agreement. For CLE, the total cell count per villi ranged from 49 to 220 and the total gap count per villi ranged from 0 to 10. In CM, the total cell count per villi ranged from 50 to 161, whereas the total gap count per villi ranged from 0 to 7. The Spearman's correlation coefficient of inter-observer cell counts was 0.90 (95% CI: 0.83, 0.94) for CLE, and 0.95 (95% CI: 0.92, 0.97) for CM. The inter-observer correlation of CLE for cell counts is shown in Figure 8. The Spearman's correlation coefficient of inter-observer gap counts was 0.86 (95% CI: 0.78, 0.91) for CLE, and 0.80 (95% CI: 0.69, 0.87) for CM. The intra-observer agreement at 1 month were: for cell counts, the Spearman's correlation coefficient were 0.99 (95% CI: 0.98, 0.99) for CLE, and 0.99 (95% CI: 0.982, 0.993) for CM; for gap counts, the Spearman's correlation coefficient were 0.94 (95% CI: 0.90, 0.96) for CLE, and 0.91 (95% CI: 0.85, 0.94) for CM. The intra-observer correlation of CLE for cell counts is shown in Figure 9.

DISCUSSION

Using confocal endomicroscopy, multi-photon confocal microscopy, and light microscopy, we performed the first validation study for a quantitative measure of the epithelial gap density in the small intestine. The magnification of all three modalities enables visualization of individual cells and epithelial gaps resulting from shedded cells. We have demonstrated that epithelial gap density, a quantitative measure of epithelial gaps in the small intestine, is closely

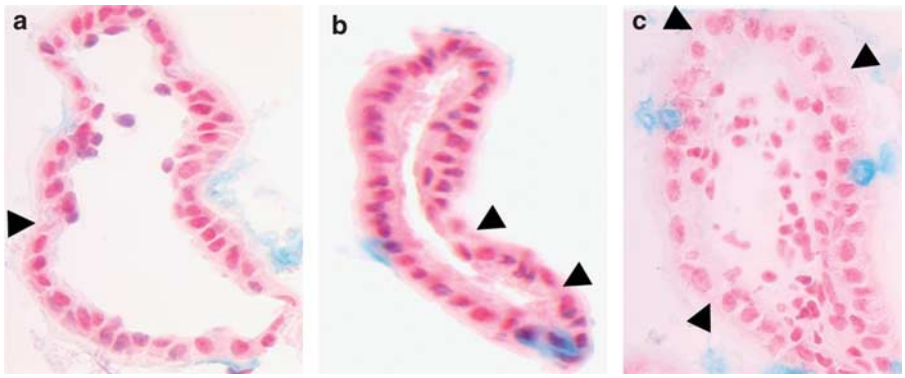

Figure 6 Representative light microscopy images of epithelial gaps in control (**a**), IL-10$^{-/-}$ (**b**), and tumor necrosis factor (TNF)-α-treated control (**c**) mice, respectively. The frozen sections of the small intestine were stained with alcian blue and nuclear fast red for identification of epithelial gaps. Black arrowheads indicate epithelial gaps observed in between cells.

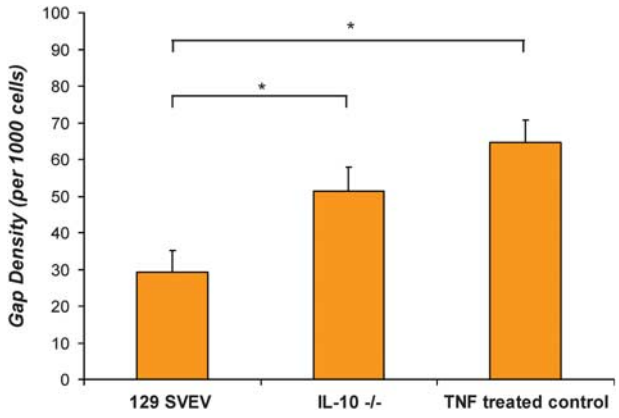

Figure 7 Epithelial gap densities for control 129 Sv/Ev, IL-10$^{-/-}$, and tumor necrosis factor (TNF)-α-treated control mice (mean values ± s.d.) using light microscopy. The *P*-values for comparison of the means were determined using Wilcoxon signed-rank test. * indicate $P < 0.0001$.

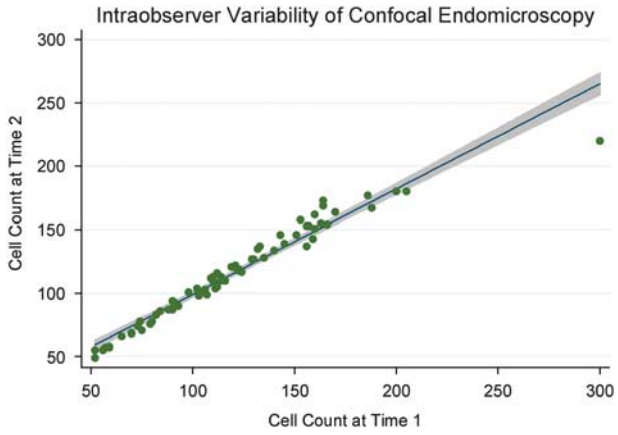

Figure 9 Intra-observer correlation of confocal laser endomicroscopy for cell counts at 1-month interval, with the 95% confidence bands is shown.

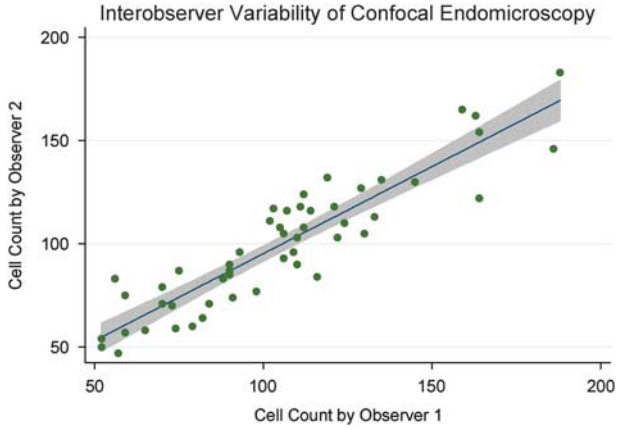

Figure 8 Inter-observer correlation of confocal laser endomicroscopy for cell counts, with the 95% confidence bands is shown.

correlated using CLE and conventional CM. We observed a twofold increase in the density of epithelial gaps in the IL-10$^{-/-}$ mice compared with the background 129 Sv/Ev strain. The acute injection of TNF-α further increased the epithelial gap density in the 129 Sv/Ev beyond the disease model. This is expected as TNF-α has been shown to acutely induce epithelial cell shedding by as much as 20-folds at 4-h post-injection. Our data suggest that increased epithelial cell shedding as demonstrated by increased epithelial gap density might represent another potential mechanism of barrier dysfunction in the pathogenesis of IBD.

The epithelial gap density from CLE and CM are closely correlated, as the determination of epithelial gaps and cells are from the 3-D reconstruction of cross-sectional 2-D images. The gap density observed with light microscopy was different than the CLE and CM because the histological images are 2-D, and 3-D reconstruction is not possible. However, the 2-D to 3-D relationship of the two morphological methods can be demonstrated by calculating the relative ratio of gap densities of IL-10$^{-/-}$ to control seen with light microscopy ($51.5/29.2 = 1.76$), to the ratio of gap densities of IL-10$^{-/-}$ to control observed on CM ($22.8/7.3 = 3.12$), which is a square relationship ($1.76\text{^}2 = 3.11$). The light microscopy represents a 2-D circle (or cross-sectional view) of the villous, whereas CLE or CM is a 3-D spherical representation of the villi, thus, the relative relationship between 2-D and 3-D epithelial gap density is a square relationship. The difference

in the gap densities observed with CLE and CM is larger for the TNF-α-treated mice, as TNF-induced epithelial cell shedding are typically patchy, resulting in a greater sampling variance in this group. Findings of our study confirms the findings of increased epithelial gap density seen in IBD patients,[14] and suggest possible mechanism for the enhanced epithelial cell shedding.

Epithelial gaps, defined as the residual spaces left by the shedding cells, may be used as a surrogate indicator of cell-shedding events, as accurate quantitation of epithelial cell shedding in patients using CLE would not be feasible. Moreover, as epithelial cell shedding is a physiological event, the development of a quantitative measure of epithelial gaps is essential for meaningful comparisons of diseased and healthy states. Epithelial gaps can be identified with special nuclear and mucin stains for frozen tissue sections, however, these methods are not readily available to clinicians. CLE, either integrated into the distal tip of a conventional endoscope (Pentax, Tokyo, Japan) or a mini-probed-based CLE unit (CellVizio, Mauna Kea Technologies, Paris, France), can be easily acquired by most endoscopy centers. Thus, clinicians can readily assess the presence of epithelial gaps during the time of endoscopy. In patients, probed-based CLE is performed at the time of colonoscopy on intact intestine, and imaging was restricted to normal appearing mucosa in the terminal ileum. Epithelial gaps appeared as white areas in between dark-appearing epithelial cells on probed-based CLE images.[13,14] This appearance was due to leakage of the intravenously administered fluorescein contrast material through the intercellular space, and can be easily identified. We speculate that the increased density of epithelial gaps might be an indicator of the underlying disease mechanism, that is, epithelial cell shedding is related to enhanced proinflammatory cytokines. The clinical significance of the increased epithelial gap density will need further investigation. In patients, we have demonstrated significantly increased epithelial gap density in Crohn's disease and ulcerative colitis compared with controls using probed-based CLE,[13,14] which appears to have some diagnostic and prognostic values. Further investigation into the clinical significance of increased epithelial gap density is warranted, as it may have implications for therapy and prognosis.

The inter- and intra-observer variability of CLE and CM for cell and gap counts appears to be excellent. Thus, an endoscopist can be trained to perform manual cell and gap counts for the determination of gap density within a relatively short period of time. As the gap density was shown to be increased in IBD patients, a validated quantitative measure of epithelial gaps might help to discern diseased from healthy states. Automated cell counting and gap counting software is an area of active research and may be available in the near future.

The main limitation of our study was that it was performed in a rodent model rather than in patients. We chose the mouse model of IBD to establish the gap density as a reliable quantitative measure for epithelial gaps for the following reason: the 3-D reconstruction of the cross-sectional images requires serial stable images for 25 cross-sections, which is almost impossible to obtain in patients because of movement artifacts. As epithelial gaps are better determined using the 3-D-reconstructed CLE and CM images, the validation against CM, which is a direct dimensional comparison, represents the most important aspect of the quantitative validation. The light microscopy examination of ileal tissue gave gap density measure in 2-D and would not be a direct comparison with the 3-D findings. Furthermore, full-thickness tissue biopsy samples from patients are much more difficult to obtain. Finally, epithelial gaps have been quantitatively studied in the rodent intestine by other investigators,[1] providing us a reference range for the gap density-measured using light microscopy. Gap density corresponds to percentage of cell spaces or positions that are epithelial gaps, as reported in previous morphometric studies. We found 2.92% cell spaces that were gaps on light microscopy, which was almost identical to the 3% previously reported.[1] Another limitation of the study is that CLE were performed on exteriorized intestinal segment rather than through the endoscope. We adopted a well-reported method of CLE in the rodent model as the images are free of motion artifacts,[3] which allowed for 3-D reconstruction of the cross-sectional images.

Overall, the data of our study suggest that that epithelial gap density—a quantitative measure of epithelial gaps is closely correlated when determined using CLE and CM. The findings of the CLE and CM are further validated using light microscopy. In a mouse model of IBD, the epithelial gap density is significantly increased in the small intestine compared with controls when examined with all three modalities.

CONFLICT OF INTEREST

Guarantor of the article: Julia J. Liu, MD.

Specific author contributions: Study concept and design, acquisition of data, analysis and interpretation of data, drafting of the manuscript, critical revision of the manuscript for important intellectual content, statistical analysis, funding, and study supervision: Julia J. Liu; generation, collection, assembly, analysis and interpretation of the data, drafting of the manuscript, and approval of the final version of manuscript: Jan K. Rudinski; generation, collection, assembly, analysis and interpretation of the data, drafting of the manuscript, and approval of the final version of manuscript: Stephanie J. Mah; generation, collection, analysis and interpretation of the data, drafting of the article, and approval of the final version of manuscript: Aducio Thiesen; generation, collection, assembly, analysis of the data, and approval of the final version of manuscript: Haiyu Bao; analysis and interpretation of the data and approval of the final version of manuscript: Pierre Boulanger; conception and design and approval of the final version of manuscript: Eytan Wine; conception and design and approval of the final version of manuscript: Richard N. Fedorak; conception and design and approval of the final version of manuscript: Karen Madsen.

Financial support: This work was supported in part by a grant (to J.J.L.) from the Canadian Institutes of Health Research/Canadian Association of Gastroenterology and a grant (R.N.F.) from the Canada Foundation for Innovations.

Potential competing interests: None.

Study Highlights

WHAT IS CURRENT KNOWLEDGE

- Epithelial gaps in the rodent small intestine resulting from shedding of epithelial cells can be visualized using confocal laser endomicroscopy.
- Epithelial cell shedding can be induced by tumor necrosis factor-alpha.
- The density of the epithelial gaps is increased in the inflammatory bowel disease mouse (IL-10 knockout) compared with control mouse (129 Sv/Ev).

WHAT IS NEW HERE

- We quantitatively validated the findings of epithelial gap density observed using the confocal laser endomicroscopy to conventional confocal microscopy and light microscopy.
- We determined the inter-observer and intra-observer variablity for the cell counts and gap counts using confocal laser endomicroscopy.

1. Watson AJ, Chu S, Sieck L *et al.* Epithelial barrier function *in vivo* is sustained despite gaps in epithelial layers. *Gastroenterology* 2005; **129**: 902–912.
2. Sato T, Vries RG, Snippert HJ *et al.* Single Lgr5 stem cells build crypt-villus structures *in vitro* without a mesenchymal niche. *Nature* 2009; **459**: 262–265.
3. Kiesslich R, Goetz M, Angus EM *et al.* Identification of epithelial gaps in human small and large intestine by confocal endomicroscopy. *Gastroenterology* 2007; **133**: 1769–1778.
4. Bullen TF, Forrest S, Campbell F *et al.* Characterization of epithelial cell shedding from human small intestine. *Lab Invest* 2006; **86**: 1052–1063.
5. Arrieta MC, Bistritz L, Meddings JB. Alterations in intestinal permeability. *Gut* 2006; **55**: 1512–1520.
6. Garrett WS, Lord GM, Punit S *et al.* Communicable ulcerative colitis induced by T-bet deficiency in the innate immune system. *Cell* 2007; **131**: 33–45.
7. Clayburgh DR, Barrett TA, Tang Y *et al.* Epithelial myosin light chain kinase-dependent barrier dysfunction mediates T cell activation-induced diarrhea *in vivo*. *J Clin Invest* 2005; **115**: 2702–2715.
8. Clayburgh DR, Musch MW, Leitges M *et al.* Coordinated epithelial NHE3 inhibition and barrier dysfunction are required for TNF-mediated diarrhea *in vivo*. *J Clin Invest* 2006; **116**: 2682–2694.
9. Turner JR, Rill BK, Carlson SL *et al.* Physiological regulation of epithelial tight junctions is associated with myosin light-chain phosphorylation. *Am J Physiol* 1997; **273**: C1378–C1385.
10. Russo JM, Florian P, Shen L *et al.* Distinct temporal-spatial roles for rho kinase and myosin light chain kinase in epithelial purse-string wound closure. *Gastroenterology* 2005; **128**: 987–1001.
11. Nenci A, Becker C, Wullaert A *et al.* Epithelial NEMO links innate immunity to chronic intestinal inflammation. *Nature* 2007; **446**: 557–561.
12. Kiesslich R, Burg J, Vieth M *et al.* Confocal laser endoscopy for diagnosing intraepithelial neoplasias and colorectal cancer *in vivo*. *Gastroenterology* 2004; **127**: 706–713.
13. Liu JJ, Madsen KL, Boulanger P *et al.* Mind the gaps: confocal endomicroscopy showed increased density of small bowel epithelial gaps in inflammatory bowel disease. *J Clin Gastroenterol* 2011; **45**: 240–245.
14. Liu JJ, Wong K, Thiesen AL *et al.* Increased epithelial gaps in the small intestines of patients with inflammatory bowel disease: density matters. *Gastrointest Endosc* 2011; doi:10.1016/j.gie.2011.01.018 (in press).
15. Arrieta MC, Madsen K, Doyle J *et al.* Reducing small intestinal permeability attenuates colitis in the IL10 gene-deficient mouse. *Gut* 2009; **58**: 41–48.
16. Madsen KL, Malfair D, Gray D *et al.* Interleukin-10 gene-deficient mice develop a primary intestinal permeability defect in response to enteric microflora. *Inflamm Bowel Dis* 1999; **5**: 262–270.
17. Bimczok D, Post A, Tschernig T *et al.* Phenotype and distribution of dendritic cells in the porcine small intestinal and tracheal mucosa and their spatial relationship to epithelial cells. *Cell Tissue Res* 2006; **325**: 461–468.
18. Musch MW, Walsh-Reitz MM, Chang EB. Roles of ZO-1, occludin, and actin in oxidant-induced barrier disruption. *Am J Physiol Gastrointest Liver Physiol* 2006; **290**: G222–G231.
19. Appleton PL, Quyn AJ, Swift S *et al.* Preparation of wholemount mouse intestine for high-resolution three-dimensional imaging using two-photon microscopy. *J Microsc* 2009; **234**: 196–204.
20. Staudt T, Lang MC, Medda R *et al.* 2,2′-Thiodiethanol: a new water soluble mounting medium for high resolution optical microscopy. *Microsc Res Tech* 2007; **70**: 1–9.